

# Description of TEAM Workshop Problem 33.b: Experimental Validation of Electric Local Force Formulations.

Olivier Barré, Pascal Brochet, *Member, IEEE*

**Abstract**— Under external stresses, the response of any material is a mechanical deformation. This paper describes an experiment whose goal is to test the accuracy of force formulations associated with an electric field. First of all, two copper plates are used to generate electric field. A specimen with high relative permittivity is set on one plate and its deformation is observed. The geometry of all parts is well described; physical properties of all materials are specified. These data allow anyone to build and model this test bench and compare calculated results with experiment.

**Index Terms**—Electric forces, Local forces, Electric fields, Experimental validation and energy methods.

## I. INTRODUCTION

When external forces are acting on a body, deformations are always encountered. But, for common materials, such deformations will remain invisible if the external stresses are very low. The electric field intensity and consequently, the local forces induced by it, are limited by the properties of the surrounding air. Hence, in this experiment, a specimen with high relative permittivity and very low Young modulus is submitted to an external electric field. With these properties, this specimen can provide visible deformation. By using material with high relative permittivity, the final strain increases. But caution is needed when a finite element model is used to calculate electric field distribution. The body geometry must not present any geometrical singularity. Knowing that the body deformation is linked to the external stress distribution, it is possible to test any local force formulation. Local force formulation associated to the energy principle is given as an example. Its universal aspect is an interesting point of view [1] [2].

## II. TEST BENCH OVERVIEW.

When a dielectric body is submitted to an external electric field, electric forces act on its boundaries [3]. Such a stress

O. Barré. is with the Laboratoire D'Electrotechnique et d'Electronique de Puissance of Ecole Centrale de Lille, Cité Scientifique, BP-48, 59651 Villeneuve d'Ascq Cedex, France (Phone : 33-03-20335385 ; Fax : 33-03-20335454 ; e-mail: [olivier.barre@ec-lille.fr](mailto:olivier.barre@ec-lille.fr)).

P. Brochet. is with the Laboratoire D'Electrotechnique et d'Electronique de Puissance of Ecole Centrale de Lille, Cité Scientifique, BP-48, 59651 Villeneuve d'Ascq Cedex, France (e-mail: [pascal.brochet@ec-lille.fr](mailto:pascal.brochet@ec-lille.fr)).

distribution induces a mechanical deformation [4] [5]. A specimen is inserted in an electric field generated by two conducting plates (Fig. 1).

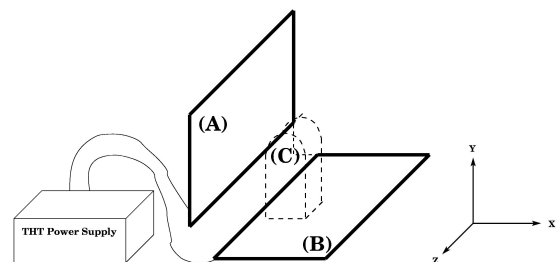


Fig. 1. Two conducting plates (A) and (B) are used to create a high electric field. A body (C), made of a dielectric substance, is submitted to this electric field and a visible deformation can be observed.

## III. ELECTRIC FIELD GENERATION.

Generating field is easy. Unfortunately, the surrounding air does not support high levels of electric field strength. In order to avoid electric arc, the difference of potential between the two conducting plates must not exceed 11 Kvolt. The geometry is given in the Fig. 2.

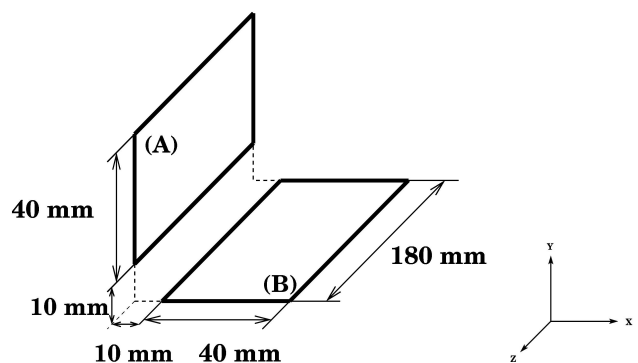


Fig. 2. Plates (A) and (B) are made of copper and their length in the Z-direction is large enough to be considered as independent of Z.

## IV. SPECIMEN.

By using dissolved gelatine in pure water, it is very easy to obtain a dielectric material presenting a very weak modulus of elasticity. But high geometrical accuracy is not so easily

obtained with such material. With a mould, the geometry of this body can be accurate; a suitable process is presented in Fig 3. Water is the most important component and the relative permittivity of this material can be assumed to be 78.5. Such a high relative permittivity can be prejudicial if the electric field distribution is calculated by means of the finite element method. Geometrical singularities are not suitable in the specimen; they strongly disturb computations [4]. Hence, the specimen geometry is given in the Fig 4.

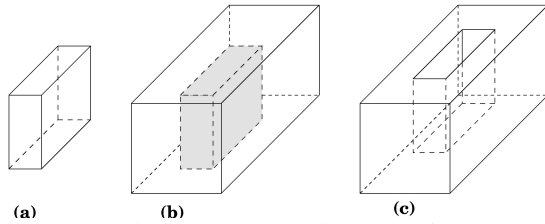


Fig. 3. With moulding method, it is possible to manufacture a body with accurate geometry. A perfect geometry (a) is used, a print of this model can be done (b) and finally, with this mould (c), it is possible to build a large number of specimens with a perfect geometry.

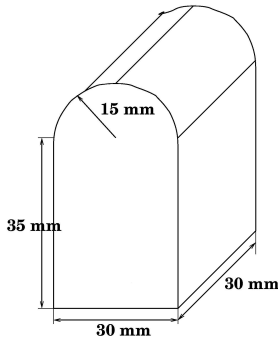


Fig. 4. Specimen geometry. The basic material is some gelatine dissolved in pure water.

V. PHYSICAL PROPERTIES OF THE TEST MATERIAL

Two physical properties are needed, since an entire simulation of this experiment is expected: relative permittivity, assumed to be equal to 78.5 and Young modulus. Moreover, for the mechanical model, the Poisson coefficient is also required. Young modulus can be measured with simple compression test. Such a framework is presented in Fig 5. Finally, repeating this experiment for several load value and also many times, curves can be plotted and an average Young modulus can be deduced (Fig. 6).

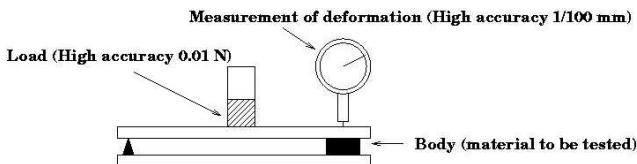


Fig. 5. Measurement of the Young modulus. The load is increased step by step and the deformation of the body is measured.

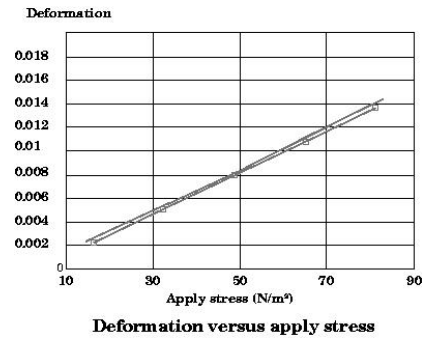


Fig. 6. With these curves, given by the compression test, the average Young modulus of the test material can be calculated. Only two curves are drawn to preserve legibility.

In conclusion, the mechanical properties for this material are 0.5 for the Poisson coefficient and 6 000 N/m<sup>2</sup> for the Young modulus.

VI. EXPERIMENTAL RESULTS.

Measurement must be done without contact and deformations are very low compared with the test bench geometry. With a camera and a macro photography lens, it is possible to observe and measure very low displacements. A fix gauge is added to the test bench and it is used as reference when measurement is needed (Fig. 7). Looking at photographs taken of the specimen, its displacement can be measured (Fig. 8).

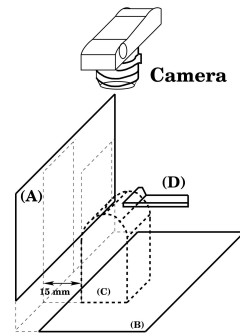


Fig. 7. Photographs of the specimen are taken with the camera. The first one is the specimen without electric field and the second one is taken when the 11 Kvolt power supply is applied. As the fix gauge is visible in the photographs, the deformation of the top of the specimen can be measured.

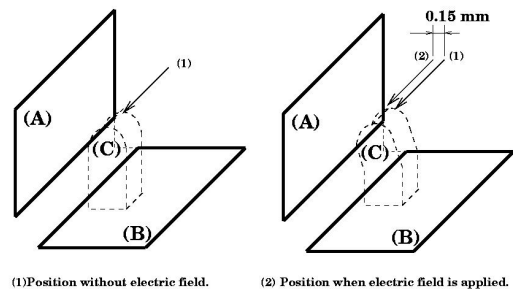


Fig. 8. The top of the specimen presents a displacement of 0.15 mm when an 11 Kvolt power supply is applied.

## VII. NUMERICAL SIMULATION OVERVIEW AND RESULTS.

A model is built in X-Y plane, the behaviour is assumed to be independent of Z. It is sure that with such simple geometry, the electric field calculation should be conducted with an optimised bounding box. However, in this example, as such optimisation is not the goal, a large volume of the surrounding air is taken into account. The structure is centred in a 0.6 m square box (Fig. 9). In the vicinity of and within the specimen, the mesh density increases (Fig. 10).

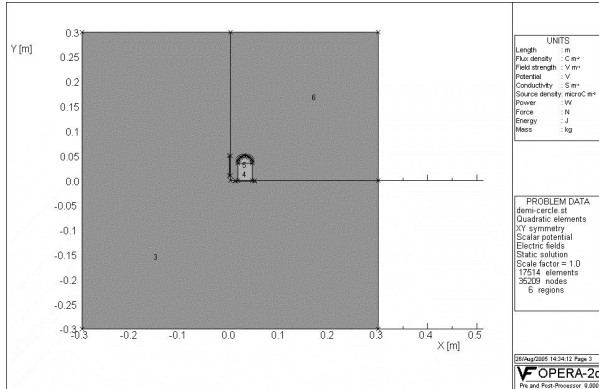


Fig. 9. The structure is studied with a large volume of surrounding air.

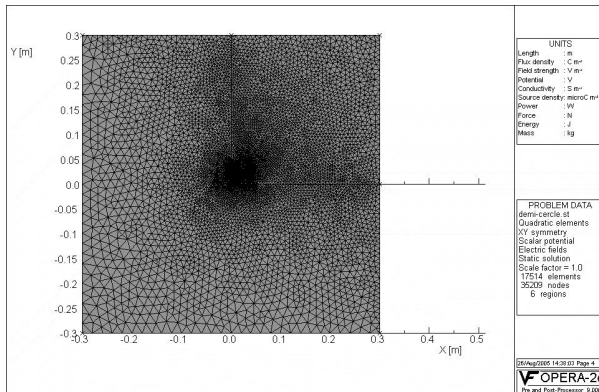


Fig. 10. Mesh density increases as soon as the test structure is reached.

High-density mesh is not required since the geometry is smooth. The selected density for simulation is presented in Fig. 11. With this mesh density, the field distribution in the surrounding air is calculated and a field plot is shown in Fig. 12. Some numerical results are given in Figs. 13,14 and 15. Applying the energy method, the local force formulation (1) associated to the electric field can be written. With the computed field distribution, the predicted stress distribution is calculated and the numerical results are given in Fig. 16.

$$\vec{F}_n = \left[ \frac{1}{2} \frac{1}{\epsilon_0} \left( 1 - \frac{1}{\epsilon_r} \right) D_n^2 + \frac{\epsilon_0}{2} (1 - \epsilon_r) E_t^2 \right] \vec{n} \quad (1)$$

A similarity must be noticed between this electric local force formulation (1) and the magnetic local force formulation associated to the energy principle [6]. First of all, considering

energy variation as a mechanical work is common at both electric and magnetic field [3] [7] [8] [9]. When two different materials are taken into account, the local forces can be expressed as a variation of permeability or as a variation of permittivity. D. Sivoukhine, in studying a very simple system, shows that such result is easily obtained in the case of magnetic field [6]. Using behaviour law and the properties of continuity for the magnetic flux or for the magnetic field, the following equation (2) is the basic result of this point of view. The force is normal and the vector  $\vec{n}$  is oriented toward the outside of the material.

$$\vec{F}_n = \left[ \frac{1}{2} \frac{1}{\mu_0} \left( 1 - \frac{1}{\mu_r} \right) B_n^2 + \frac{1}{2} \mu_0 (1 - \mu_r) H_t^2 \right] \vec{n} \quad (2)$$

With behaviour laws associated to electric field and also the properties of continuity for the electric field or for the electric source field, equation (1) can be deduced from equation (2).

As the base of this specimen is fixed on the plate, displacement associated to nodes 0 and 46 are equal to 0 and local forces associated to this node do not induced deformation for the whole structure. Local forces attached to these nodes can be also set to 0. Calculation of mechanical displacement can be solved with finite element method. As this problem has been presented as a 2D problem, it can be solve with any mechanical software that used finite element resolution. Information about such resolution can be found in several books or software documentation [10] [11] [12] [13].

Finally, the stress distribution associated to the energy method gives a deformation with the top of the specimen having a displacement of 0.1425 mm (Fig. 17).

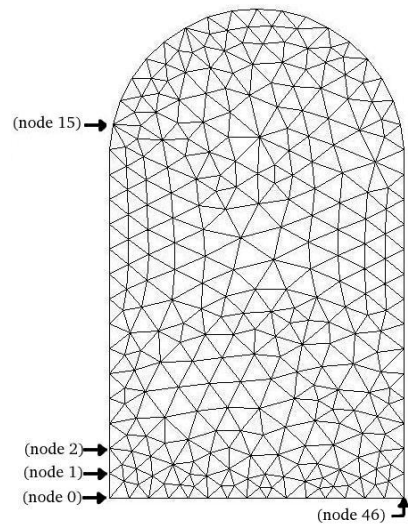


Fig. 11. Mesh density of the specimen is the same in the electric field and mechanical studies. Nodes on the boundary are numbered from 0 to 46. There are 14 equal segments on the two vertical borders; consequently 15 nodes are built on these two borders. The top is cut out into 18 equal segments; it brings the last 17 nodes.

## VIII. CONCLUSION.

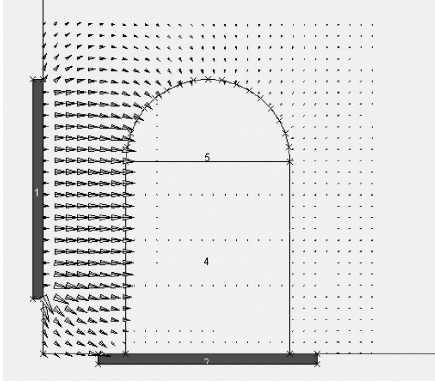
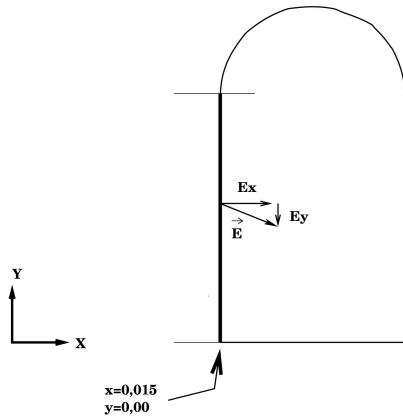


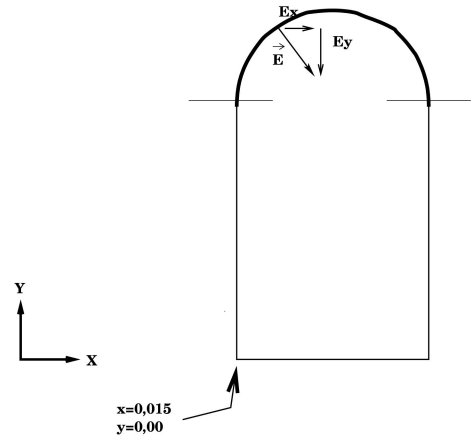
Fig. 12. Electric field distribution in the surrounding air of the specimen.

A material with low Young modulus is not usual in electro-magnetic devices. It sometimes has some interesting properties, such as providing visible deformation under low external stress. Such properties are advantageously used in this test bench. The local force formulation associated to the energy principle is the only formulation that has been tested but many other formulations can be evaluated. The geometry of the specimen is quite simple but more sophisticated geometries can also be used as soon as they can be obtained by the manufacturing process presented in section IV. Finally many other experiments, based on this material, can be produced and using electric field in place of magnetic field in studies should be a valuable approach.



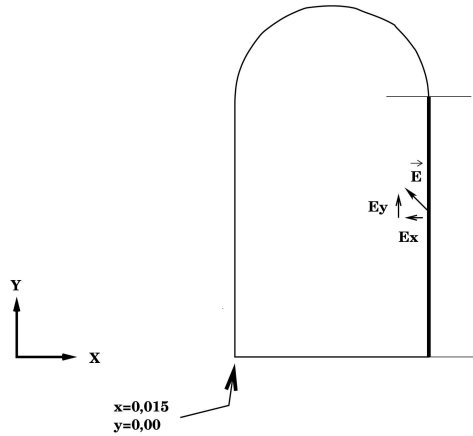
Position:			
X (m)	Y (m)	Ex (V/M)	Ey (V/M)
0.0149	0	463.47	45226.8
0.0149	0.0025	217148	-29933.3
0.0149	0.005	369255	-24928.4
0.0149	0.0075	468404	-22443.7
0.0149	0.01	540831	-20197
0.0149	0.0125	594318	-18275.1
0.0149	0.015	633590	-16306.2
0.0149	0.0175	660241	-14779
0.0149	0.02	678030	-13357.9
0.0149	0.0225	689355	-12022.6
0.0149	0.025	697297	-10967.2
0.0149	0.0275	704113	-10035.6
0.0149	0.03	712641	-9311.64
0.0149	0.0325	729604	-9011.96
0.0149	0.035	792987	-44685.1

Fig. 13. Some numerical values for the electric field intensities along x and y references associated to a line at the left boundary of the specimen.



Position:			
X (m)	Y (m)	Ex (V/M)	Ey (V/M)
0.015015	0.0364	774786	-78743.4
0.015465	0.038965	738744	-198452
0.016355	0.041415	633316	-293758
0.01766	0.04367	500857	-342072
0.019335	0.045665	363694	-351463
0.02133	0.04734	245102	-335389
0.023585	0.048645	152071	-306379
0.026035	0.049535	80067	-272081
0.0287	0.050885	36718	-222156
0.0313	0.050885	-660.14	-192417
0.033965	0.049535	-39018.8	-164317
0.036415	0.048645	-58547.8	-134959
0.03867	0.04734	-69935.4	-107485
0.040665	0.045665	-76298.9	-82938
0.04234	0.04367	-78644.6	-61407
0.043645	0.041415	-77559.7	-42119
0.0445	0.038965	-73269.6	-25367
0.044985	0.0364	-63870.3	-11872

Fig. 14. Some numerical values for the electric field intensities along the top of the specimen.



Position:

X (m)	Y (m)	$E_x$ (V/M)	$E_y$ (V/M)
0.0451	0	-83.58	17056
0.0451	0.0025	-23444.3	-14397.4
0.0451	0.005	-36540.7	-13699.2
0.0451	0.0075	-41383.4	-13104.9
0.0451	0.01	-42647.6	-12609.1
0.0451	0.0125	-42521.6	-12128
0.0451	0.015	-42036.2	-11629.8
0.0451	0.0175	-41605.2	-11098
0.0451	0.02	-41433.2	-10539.4
0.0451	0.0225	-41682.2	-9931.02
0.0451	0.025	-42430.6	-9313.86
0.0451	0.0275	-43918.8	-8650.63
0.0451	0.03	-46391.6	-7953.75
0.0451	0.0325	-50733.2	-7258.29
0.0451	0.035	-60327.9	-8945.98

Fig. 15. Some numerical values for the electric field intensities along x and y references associated to a line at the right boundary of the specimen.

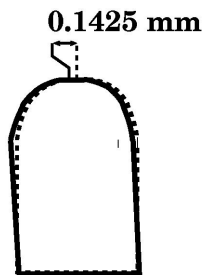
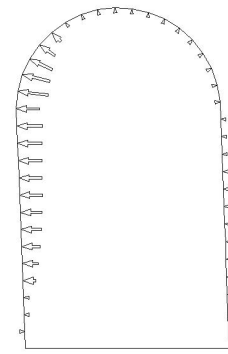


Fig. 17. Deformation associated to the load case presented in Fig. 16.



Node number	Force (N/M)	
	X Component	Y Component
0	0.000e+00	0.000e+00
1	2.252e-04	0.000e+00
2	-9.550e-04	0.000e+00
3	-1.962e-03	0.000e+00
4	-2.841e-03	0.000e+00
5	-3.567e-03	0.000e+00
6	-4.151e-03	0.000e+00
7	-4.568e-03	0.000e+00
8	-4.862e-03	0.000e+00
9	-5.060e-03	0.000e+00
10	-5.201e-03	0.000e+00
11	-5.322e-03	0.000e+00
12	-5.466e-03	0.000e+00
13	-5.733e-03	0.000e+00
14	-5.150e-03	0.000e+00
15	-6.787e-03	7.830e-04
16	-6.056e-03	1.436e-03
17	-5.040e-03	2.360e-03
18	-3.403e-03	2.383e-03
19	-2.019e-03	2.019e-03
20	-1.097e-03	1.565e-03
21	-5.440e-04	1.161e-03
22	-2.210e-04	8.360e-04
23	-2.790e-05	3.157e-04
24	1.600e-05	1.810e-04
25	7.900e-05	2.980e-04
26	9.800e-05	2.090e-04
27	9.700e-05	1.390e-04
28	8.800e-05	8.800e-05
29	7.300e-05	5.100e-05
30	5.700e-05	2.700e-05
31	1.300e-05	3.000e-06
32	2.900e-05	0.000e+00
33	-2.490e-04	0.000e+00
34	-1.710e-04	0.000e+00
35	-3.000e-05	0.000e+00
36	-4.300e-05	0.000e+00
37	-5.400e-05	0.000e+00
38	-6.500e-05	0.000e+00
39	-7.600e-05	0.000e+00
40	-8.600e-05	0.000e+00
41	-9.600e-05	0.000e+00
42	-1.060e-04	0.000e+00
43	-1.280e-04	0.000e+00
44	-1.460e-04	0.000e+00
45	-1.710e-04	0.000e+00
46	0.000e+00	0.000e+00

Fig. 16. Local Force intensities, associated to the energy principle, induced by the electric field on the surface of the specimen. These values are used as load case in the mechanical calculation.

## REFERENCES

- [1] J. Penman, J.R. Fraser, "Complementary and dual energy finite element principles in magnetostatics", IEEE Transaction on magnetics, Vol. 18, N°2, March 1982, pp 319-324.
- [2] C. Li, Z. Ren, A. Razek, "Complementarity between the energy results of H and E formulations in eddy-current problems", Science, Measurement and technology. IEE proceeding A, issue 1 januray 1994, pp 25-30.
- [3] J.D. Jacobson, H.S. Goodwin-Johansson, "Integrated force arrays: Theory and modelling of static operation", IEEE journal of microelectromechanical systems, Vol. 4, N°3, September 1995, pp 139-150.
- [4] O.Barré, P. Brochet, "Geometrical singularities effects on the calculation of the magnetic forces studied by an equivalent behaviour approach", in: SSD'05, 3rd International Conference on Systems, Signals & Devices, Sousse, Tunisia, 21-24 mars 2005.
- [5] O. Barré, P. Brochet, M. Hecquet, "Experimental validation of magnetic and electric local force formulations associated to energy principle", In Proceeding of the COMPUMAG 2005 conference, in Shenyang, Liaoning, (China), 26-30 June 2005.
- [6] D. Sivoukhine, "Cours de physique générale- tome 3 – électricité", "General physics courses- volume 3 – Electricity", 1983 "Mir" Publisher. <http://www.urss.ru>
- [7] Z. Ren, "Comparison of Different Force Calculation Methods in 3D Finite Element Modelling", IEEE Transaction on magnetics, Vol. 30, N°5, September 1994, pp 3471-3474.
- [8] G.Reyne, J.C. Sabonnadière, J.L. Coulomb, P. Brissonneau., « A Survey of The Main Aspects of Magnetic Forces and Mechanical Behaviour Of Ferromagnetic Materials Under Magnetisation », ", IEEE Transaction on magnetics, Vol.. MAG-23, N°5, September 1987, pp 3765-3767.
- [9] Z. Ren, Z. Cendes, ., «Shell Elements for the Computation of Magnetic Forces », ", IEEE Transaction on magnetics, Vol.. 37, N°5, September 2001, pp 3171-3174.
- [10] Ansys 10.0 Documentation, Ansys Inc Theory Reference.
- [11] J. L. Batoz, G. Dhatt, "Modélisation des structures par éléments finis", Volume 1, Solides élastiques, Hermes edition 1990.
- [12] J. N. Reddy, « Introduction to the Finite Element Method », McGraw-Hill, New York (1993).
- [13] O. C. Zienkiewicz, R. L. Taylor, « The Finite Element Method », McGraw-Hill, New York (2000)